Effect of Poly(ethylene methyl acrylate) Copolymer on Thermal, Morphological, and Mechanical Properties of Polypropylene Copolymer Blown Films

Giri Gururajan,[1] Victoria Froude,[1] Stephen Riutta,[1] Aline Thomas,[1] Ian Gao,[1] S. L. Samuels,[2] D. F. Massouda,[2] M. Weinberg,[2] A. A. Ogale[1]

[1]*Department of Chemical and Biomolecular Engineering and Center for Advanced Engineering Fibers and Films (CAEFF), Clemson University, Clemson, South Carolina*
[2]*Central Research and Development, DuPont Company, Wilmington, Delaware*

Received 21 May 2007; accepted 4 September 2007
DOI 10.1002/app.27275
Published online 9 November 2007 in Wiley InterScience (www.interscience.wiley.com).

ABSTRACT: Blends of polypropylene copolymer (PP-cp) and poly(ethylene methyl acrylate) [poly(EMA)] copolymer blends were processed by blown film extrusion. The orientation and crystallinity of PP-cp matrix in the blend did not change significantly with the addition of EMA. The low machine direction and transverse direction tear strengths, which are observed for neat polypropylene blown films more than doubled at 6 wt % or higher content of EMA. The increase in tear properties was mainly attributed to a fine dispersion of EMA in the matrix with an average particle size of 100–500 nm and the formation of elongated domains. The dispersed nonrounded EMA domains, resulting from the blown-film process, enhance better energy dissipation mechanism with the formation of an extended plastic zone in the blend films as compared with that in pure PP-cp films. © 2007 Wiley Periodicals, Inc. J Appl Polym Sci 107: 2500–2508, 2008

Key words: polypropylene copolymer; poly(ethylene methyl acrylate); blend; blown film; tear resistance

INTRODUCTION

Polypropylene (PP) is a high-volume polyolefin widely used to produce blown films.[1] Although PP films offer excellent strength and abrasion resistance, they possess low impact strength. Anisotropic tear properties are often the cause, since the film fails in the weakest direction upon impact or puncture. To overcome these problems, impact polypropylene copolymer (PP-cp) has been introduced, in which an elastomer is incorporated during polymerization. However, the elastomeric content is constrained by the polymerization-controlled process. Therefore, compounding of PP with miscible or immiscible elastomeric copolymers such as ethylene–octene copolymer, ethylene–propylene copolymer (EPR), ethylene–propylene–diene terpolymer, and poly(ethylene vinyl acetate) is being explored to improve properties.[2–5]

Commercial grades of ethylene methyl acrylate (EMA) copolymers are available in a range of comonomer contents [5–35 wt % methyl acrylate (MA)] that display characteristics ranging from thermoplastic response at low MA content to elastomeric/rubbery behavior at higher MA contents.[6] EMA offers an advantage over other copolymers in that it possesses excellent thermal stability and can be processed with PP at high temperatures.[7] Genovese and Shanks[8,9] investigated the thermal and tensile properties of different compositions of EMA/PP obtained by slit-die extrusion. Their study reported poor compatibility of EMA with PP at 16.5 wt % or higher MA content, because of its high polarity and lack of interactions between the components.

However, due to the presence of ethylene in its backbone structure, EMA is highly compatible with polyethylene. Santra et al.[10] reported EMA as a good compatibilizer for blends containing low-density polyethylene (LDPE) and polydimethylsiloxane (PDMS) rubber. At 6 wt % EMA in the LDPE/PDMS blend, they found a significant increase in adhesion between the components and improved impact strength of the blend.

Morphological, rheological, and thermal behavior of PP blended with various elastomers has been reported in prior literature studies.[11–13] The properties of the elastomer blends are typically controlled by the type and concentration of the components,[14] interparticle distance, domain size[15] and shape,[16] matrix morphology of the blends,[17] and interaction between the components. The domain size of the dispersed phase is indicative of the compatibility of the blend systems, i.e., the smaller the domain size,

Correspondence to: A. A. Ogale (ogale@clemson.edu).
Contract grant sponsor: National Science Foundation (The Engineering Research Centers Program); contract grant number: EEC-9731680.

the more compatible are the components and better are the mechanical properties.[18] In some cases, compatibilizers are used to obtain finer dispersion of domains of the elastomers, and thereby improved mechanical properties.[18,19] The size and shape of the dispersed domains is controlled by the viscosity ratio of the dispersed phase to the matrix, shear rate, interfacial tension, temperature, concentration, and the draw ratio.[20] Of these factors, viscosity ratio, shear stress in the die, and draw ratio are more relevant during the blown film extrusion.

Various literature studies have reported on the mechanical properties of blends of homo-PP with various elastomers, but only limited studies have reported on the properties of blends of PP-cp with elastomers.[5,21] Also, the processing of PP-cp/EMA blends into blown films and the study of the process-dependent tear property has not been extensively reported. Though low-speed tensile tests and high-speed impact tests are mostly performed on polymeric blends made from different molding techniques, high-speed tear tests are more relevant to evaluate the performance of the films.

The tear properties of single-component films of PP, LDPE, and HDPE have been explained on the basis of crystalline morphology and orientation,[22–24] while the tear strength of immiscible blend films or sheets has been explained based on the size of the dispersed domains,[25–28] interfacial adhesion,[26] and interparticle distance.[29] To the best of our knowledge, only a few studies have reported on the effect of the shape of the dispersed domains on the tear properties of the blend films.[30] Therefore, the purpose of the present study was to investigate the effect of various contents of EMA copolymer on the thermal and tear behavior of PP-cp blown films. We used wide-angle X-ray diffraction (WAXD) technique to measure any change in crystallinity and orientation of the PP-cp matrix due to the presence of EMA. We present transmission electron microscopy (TEM) observations that help in better understanding of the mechanical properties of the PP-cp/EMA blend in the context of the blown film process.

EXPERIMENTAL

Materials and processing

PP-cp (Inspire D 114, 0.9 g/cc and 0.5 g/10 min MFI, Dow Chemical, Midland, MI) and an EMA copolymer (Entira™ Strong polymer modifier, DuPont Company, Wilmington, DE) were used throughout this study. As reported in the literature,[31] the PP-cp contained 4–10 wt % of EPR. EMA used in this study is a random copolymer containing over 18 wt % of methyl acrylate.

PP-cp and EMA pellets were physically blended and fed to the extruder hopper to form blown films of five different compositions: 0, 2, 6, 15, and 100 wt % EMA. The addition of EMA to PP-cp generally helped to improve the processability and stability of the bubble. A total mass flow rate of 36 g/min and die temperature of 240°C was maintained throughout the experiment. The single-lip air ring generated an air velocity of 20 m/s at the lip. All films were processed at a blow-up ratio of 1.7 and a take-up ratio of 3.5.

Mechanical testing

Tensile tests were performed using a SATEC tensile testing machine on 100 wt % PP-cp, PP-cp/2wt % EMA, PP-cp/6wt % EMA, PP-cp/15 wt % EMA, and 100 wt % EMA films according to the ASTM D 882 standard. Ten replicates were tested in machine direction (MD) and transverse direction (TD). Tear resistance testing was also performed on these films using Elmendorf tear testing machine according to the ASTM D 1922-03a procedure. A nominal thickness of 125 μm was maintained for all film samples during testing. Tear resistance was calculated in the units of N/mm required to propagate tearing across the film samples from a 20-mm precut slit. Thirty samples were tested for each composition and error bar represents 95% confidence intervals.

X-ray diffraction and birefringence

Wide-angle X-ray diffraction measurements were obtained in the transmission mode from a Rigaku 2D diffractometer (Rigaku/MSC, 45 kV, 0.67 mA) using CuK_α radiation. The images were then analyzed using POLAR® software for calculating Herman's orientation factor. In-plane (Δn_{12}) and out-of-plane (Δn_{13}, Δn_{23}) birefringence values were measured using an optical microscope (BX-60F5, Olympus Optical, Japan) fitted with cross-polarizers and U-TCB Berek compensator using the method described by Stein.[32] For PP-cp/EMA blend films, the birefringence from PP component was determined based on the rule of mixing,

$$\Delta n_{\mathrm{TOTAL}} = \Phi_{\mathrm{PP-cp}} \cdot \Delta n_{\mathrm{PP-cp}} + \Phi_{\mathrm{EMA}} \cdot \Delta n_{\mathrm{EMA}}$$

where $\Phi_{\mathrm{PP\text{-}cp}}$ and Φ_{EMA} are the volume fractions of PP-cp and EMA, respectively.

Thermal analysis

A Pyris I differential scanning calorimeter (Perkin–Elmer, Wellesley, MA) was used to measure the melting point (T_m), crystallization point (T_c), and enthalpy of crystallization (ΔH_c) of neat EMA, neat PP-

cp and PP-cp/EMA blend films. The nonisothermal scans consisted of heating from 25 to 190°C at a rate of 10°C/min (N_2 environment), holding at 190°C for 1 min, and cooling to 25°C at 10°C/min. With prior thermal processing history erased, the samples were reheated to 190°C at a rate of 10°C/min. The crystallinity of the continuous phase (PP-cp) and dispersed phase (EMA) were calculated using heat of fusion values of 139 and 293 J/g for PP-cp[33] and PE,[34] respectively. Ten samples were tested for each composition.

Morphology

Field emission scanning electron microscope (FE-SEM, Hitachi *S*-4700) was employed to study the texture of fracture surface and dispersion of EMA in the blend films, after cryogenically fracturing the machine direction–normal direction (MD–ND) cross section. SEM was conducted at low voltage (2.5 kV) in the back-scattered electrons image (BEI) mode without coating the samples to avoid any potential damage to the soft EMA domains due to heating. TEM was carried out using TEM-Hitachi H7600T. The transverse direction–normal direction (TD–ND) cross section of the films was cryomicrotomed to 60-nm thick samples at −60°C and then stained with ruthenium tetroxide for 24 h to provide enhanced contrast between EMA and PP-cp. An optical microscope (BX-60F5, Olympus Optical, Japan) fitted with cross-polarizers was used to examine the region near tear in MD–TD plane in the tear-fractured samples.

Rheological testing

Rheological measurements were carried out on the processed blown films using ARES Rheometer (TA Instruments) with parallel plate fixtures (25-mm diameter) with a gap of 0.75 mm. The steady shear viscosity measurements were conducted on pure PP-cp, pure EMA, and 15 wt % EMA blend at 240°C in the shear rate range from 0.001 to 1 s^{-1}.

RESULTS AND DISCUSSION

Mechanical properties

Tensile stress–strain curves in the low-strain zone for pure PP-cp and its EMA blends are displayed in Figure 1(a,b) for MD and TD, respectively. Neat PP-cp showed a high yield stress and a sharp decrease in stress after necking. The extent of decrease of the stress after yield is severe in TD as compared to that in the MD. This decrease was also observed in earlier studies by Chang et al.[35] This is generally observed in polyolefins like LLDPE,[34] which have

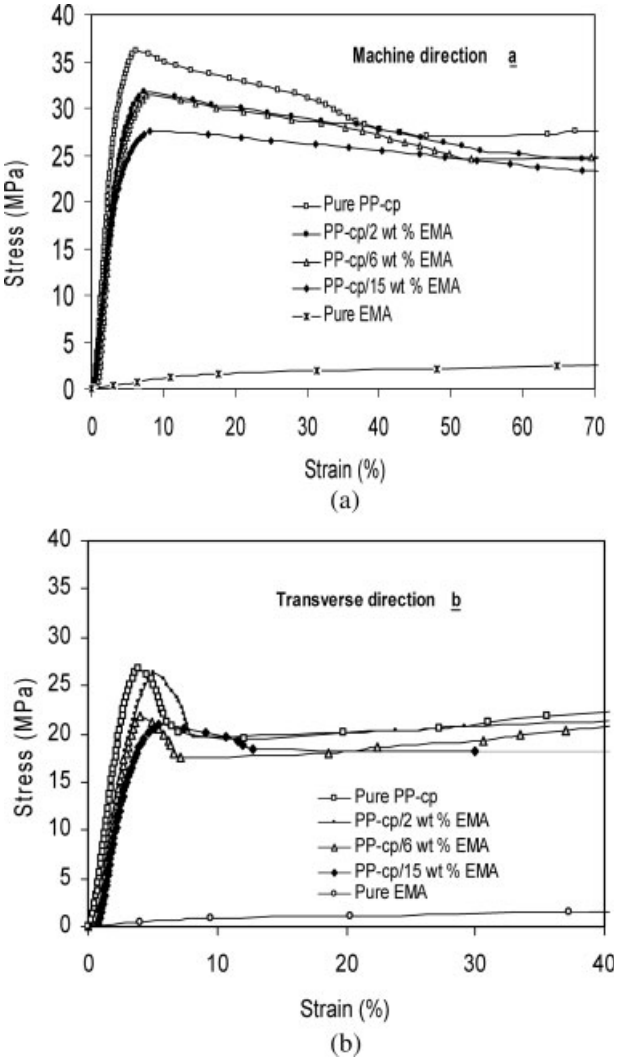

Figure 1 Typical tensile stress–strain curves in the low-strain region of PP-cp/EMA film (a) Machine direction (b) Transverse direction.

row-nucleated microstructure. The application of a tensile stress along the MD leads to deformation of the amorphous tie-chains located between lamellar stacks, because these tie-chains are much more compliant than the crystalline lamella.

In contrast to neat PP-cp, neat EMA films exhibited a gradual yielding behavior. At 15 wt % EMA in PP-cp, tensile curves in MD and TD show that blend films showed a visibly larger yield zone than neat PP-cp. Thus, significant differences were observed at low strains. The yield stress, elastic modulus, and tensile strength for different blend films are summarized in Table I. The yield stress and tensile strength of the films decreased with increasing EMA content in the blend, because of the additive effect. The strain-to-failure values did not show a statistically significant difference up to 15 wt % EMA in PP-cp.

TABLE I
Tensile Properties of PP-cp/EMA Films from Experiment and Model-Prediction in the Machine Direction (MD) and Transverse Direction (TD)

Film		Modulus (MPa)			Yield strength (MPa)	Tensile strength (MPa)
		Measured	Predicted parallel model	Predicted series model		
Pure PP-cp	MD	1340 ± 148	–	–	36.1	39.5
	TD	1555 ± 139	–	–	28.5	31.1
2 wt % EMA	MD	1105 ± 43	1313	351	32.2	36.9
	TD	1210 ± 40	1523	280	29.1	29.8
6 wt % EMA	MD	985 ± 115	1260	142	31.9	37.7
	TD	1100 ± 151	1462	106	24.9	26.7
15 wt % EMA	MD	900 ± 41	1141	61	30.5	32.2
	TD	985 ± 87	1323	44	21.7	22.1
Pure EMA	MD	9.4 ± 1.9	–	–	1.9	6.1
	TD	6.8 ± 1.2	–	–	1.6	5.2

Bounds on moduli of two-component materials may be obtained based on a two-phase model such as that used for composite materials.[36] The upper limit on the modulus can be obtained from a parallel model, $E_{\text{Blend (parallel)}} = E_A\Phi_A + E_B\Phi_B$, whereas, the lower bound can be obtained from a series model, $E_{\text{Blend (series)}} = E_AE_B/(\Phi_AE_B + \Phi_BE_A)$.[36] A comparison of experimental moduli of PP-cp/EMA films with that of the calculated bounds indicated that the blend films followed the simple rule of mixing more closely with only a slight negative deviation. This indicates that the two phases have good mechanical compatibility at low strains and the adhesion between the blend components is good enough to provide efficient stress transfer, similar to that reported in the literature for other blends.[37,38] The modulus values followed the Coran-Patel model, $E_{\text{Blend}} = fE_{\text{Blend (parallel)}} + (1 - f)E_{\text{Blend (series)}}$ with an f value of about 0.75, indicating a large fraction of parallel connection of the two phases.[36]

Next, the high strain-rate tear-resistance data are presented in Table II for MD and TD. Neat PP-cp films possessed low tear strength in the range of 2–6 N/mm with a slight anisotropy (MD < TD). It is well known that, due to its shish-kebab morphology, PP fails preferentially along the MD with the tear force propagating parallel to the crystal stems between the adjacent lamellar stacks.[39] In contrast, neat EMA films possessed not only very large tear strength values of 36–40 N/mm (~10–15 times neat PP-cp) but also balanced MD and TD values. With the addition of 2 wt % EMA in PP-cp, the tear strength of the film did not change significantly as compared to that of neat PP-cp film. But, as the EMA content increased to 6 wt %, there was a significant increase in MD and TD tear strength. MD and TD tear strengths increased about six-fold with values in the range of 10–25 N/mm at 15 wt % EMA. Experimental tear strength values were larger than those from a simple, linear mixing rule. Various microstructural factors that influence the blend properties are reported in the following sections.

Orientation and crystallization of PP

The WAXD diffractograms for various compositions are presented in Figure 2. No significant difference in the (110), (040), and (130) peaks was observed with the addition of up to 15 wt % EMA to PP-cp. The PP-cp crystalline orientation parameters calcu-

TABLE II
Tear Properties of PP-cp/EMA Films from Experiment and Linear Mixing Rule in the Machine Direction (MD) and Transverse Direction (TD)

Film		Tear strength (N/mm) measured	Tear strength (N/mm) mixing rule	MD/TD tear
PP-cp	MD	2.2 ± 1.7	2.2	0.35
	TD	6.2 ± 1.9	6.2	
2 wt % EMA	MD	4.2 ± 2.0	2.9	0.57
	TD	7.4 ± 1.6	6.9	
6 wt % EMA	MD	9.3 ± 2.9	4.3	0.93
	TD	10.0 ± 2.5	8.4	
15 wt % EMA	MD	12.8 ± 4.3	7.3	0.51
	TD	25.2 ± 7.5	11.6	
EMA	MD	36.1 ± 7.7	36.1	0.87
	TD	41.6 ± 6.7	41.6	

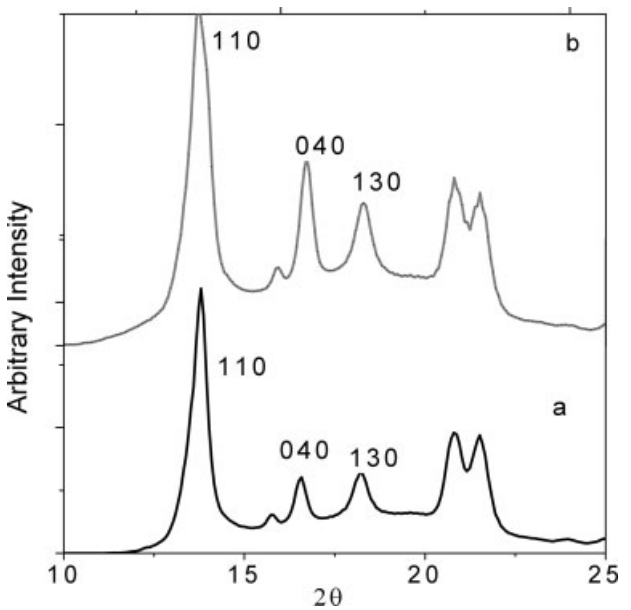

Figure 2 Wide angle X-ray diffractograms of (a) pure PP-cp film and (b) PP-cp/15 wt % EMA film.

lated from X-ray patterns using (110), (040), and (130) peaks are presented in Table III. Under the low-stress condition used in this study, the *b*-axis (040) is perpendicular to the MD, whereas the *a*-axis and *c*-axis were tilted at angle in the MD–TD plane. Crystalline orientation factors (f_a, f_b, f_c) of neat PP-cp and 15 wt % EMA blend film did not show a significant difference.

Also shown in Table III are the birefringence values of the films. Δn_{13} and Δn_{23} values were positive, and Δn_{13} was greater than Δn_{23}, indicating higher MD orientation of the polymer chains for the conditions studied. No significant differences were noted between neat and blend films. Therefore, the presence of 15 wt % EMA in PP-cp did not significantly affect the birefringence of the films, suggesting that the mechanical properties of the blends were mainly affected by factors other than molecular orientation.

Figure 3(a,b) displays the heating and cooling curves from DSC scans for different compositions of PP-cp/EMA blends. The melting point (T_m), crystallization temperature (T_c), and degree of crystallinity (X_c) for various samples obtained from nonisothermal DSC scans are summarized in Table IV. The T_c of PP-cp in PP-cp/EMA blend films decreased slightly with an increase in EMA content, suggesting that EMA decreased the nucleation rate. The T_m and X_c obtained from the endotherms did not show a significant difference compared to the respective values for neat PP-cp samples.

From the results of thermal characterization and orientation measurements, we can infer that there is high crystallinity (≈ 52 wt %) and preferential orientation of molecular chains in PP-cp compared to low crystallinity (≈ 5 wt %) and also low molecular orientation in neat EMA. These microstructural features resulted in large tear strength values observed for neat EMA films. The balanced MD and TD tear strengths is a good indicator of the equibiaxial nature of the EMA film as also supported by the birefringence values ($\Delta n_{13} \approx \Delta n_{23}$).

Morphology of blends

The optical micrographs presented in Figure 4(a,b) show the torn edges of films of neat PP-cp and 15 wt % EMA blend films, respectively, observed under cross-polarized transmitted light. Regions enclosed by the rectangular boxes represent the yield zone during failure in the MD–TD plane. The image of tear-tested neat PP-cp film [Fig. 4(a)] shows a negligible yielding with a sharp stress-whitened zone. In contrast, the blend film containing 15 wt % EMA [Fig. 4(b)] shows ruffled edges indicating substantially wider deformation than the length of the tear. So, the addition of EMA led to an increase in the yield zone, thereby drawing the domains during tear propagation. This yielding and drawing phenomenon has been related to the amount of energy the material can dissipate during the tearing process.[40] The wider the yield zone, the higher tear energy (strength) the film possesses. For a low EMA content, the film does not yield much as observed by the sharp drop of the stress in the tensile tests. However, at 15 wt % EMA, the blend films undergo substantial drawing at the tear edge, which is consistent with the large gradual yielding region observed in tensile tests.

TABLE III
Herman' Orientation Factors (f_a, f_b, f_c) from WAXD and In-Plane (Δn_{12}) and out-of-plane (Δn_{13}, Δn_{23}) birefringences of PP-cp/EMA films

			Birefringence × 10^3			Herman's orientation factor		
Polymer	BUR	TUR	Δn_{12}	Δn_{13}	Δn_{23}	f_a	f_b	f_c
Pure PP-cp	1.6	3.3	3.70 ± 0.15	5.71 ± 0.27	2.01 ± 0.30	0.11	−0.21	0.10
PP-cp/15 wt % EMA	1.6	3.3	3.48 ± 0.43	6.06 ± 0.69	2.58 ± 0.48	0.08	−0.21	0.13
Pure EMA	1.6	3.3	0.15 ± 0.03	0.52 ± 0.08	0.37 ± 0.07			

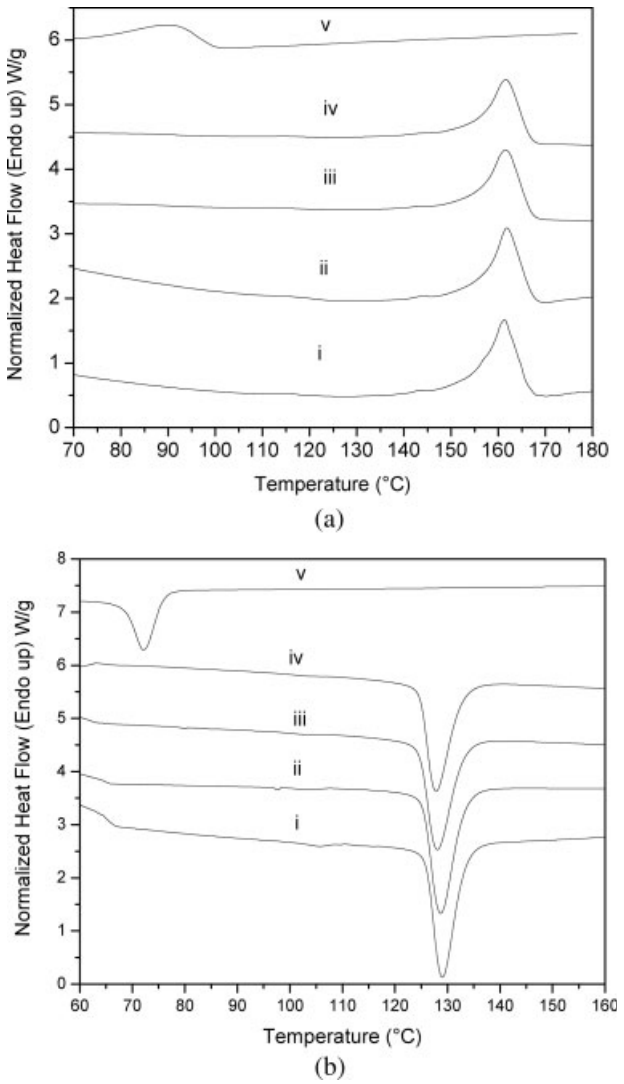

Figure 3 DSC scans for PP-cp/EMA blends: (a) Heating curves and (b) Cooling curves. The curves are stacked for clarity: i, pure PP-cp; ii, PP-cp/2 wt % EMA; iii, PP-cp/6 wt % EMA; iv, PP-cp/15 wt % EMA; v, Pure EMA.

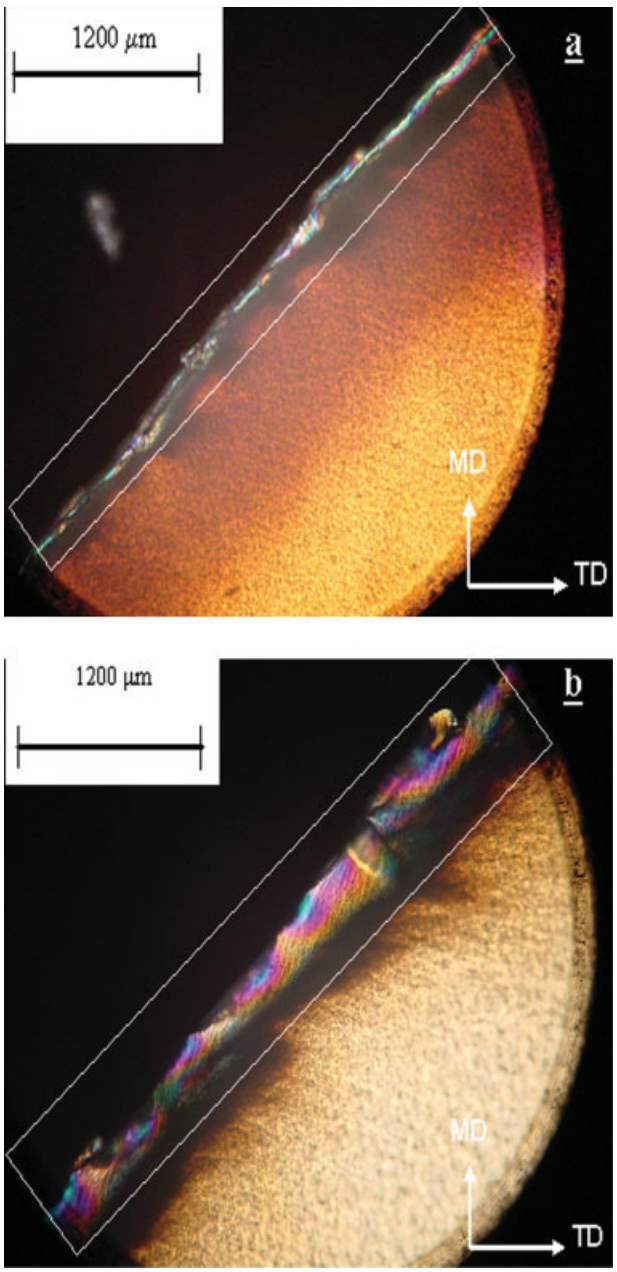

Figure 4 Optical microscopic images of the tear-tested films of (a) pure PP-cp and (b) PP-cp/15 wt % EMA under cross-polarized light [Color figure can be viewed in the online issue, which is available at www.interscience.wiley.com.]

The SEM images of cryofractured MD–ND cross sections are displayed in Figure 5 for films containing 0 and 15 wt % EMA. Figure 5(a) displays a typical fracture surface of neat PP-cp, which is relatively smooth and featureless, indicating a nonductile failure. In contrast, the micrograph for PP-cp/EMA blend [Fig. 5(b)] shows a two-phase morphology, with prominent rubbery elongated EMA domains (encircled) within PP-cp continuous phase. Further, the detachment of the domains from the matrix does not create significant voids, which has been reported as an indication of good interfacial adhesion between the dispersed and the continuous phases.[41–43]

TABLE IV
Nonisothermal Properties of PP-cp and Blends

Sample	T_c (°C)	Crystallinity (%)	T_m (°C)
Pure PP-cp	129.0 ± 0.2	49.4 ± 0.8	162.7 ± 1.2
2 wt % EMA	128.0 ± 0.2	53.9 ± 0.3	160.7 ± 0.5
6 wt % EMA	128.8 ± 0.7	51.9 ± 1.4	160.7 ± 0.8
15 wt % EMA	127.8 ± 0.1	52.2 ± 2.2	161.1 ± 0.6
Pure EMA	76.2 ± 3.0	5.3 ± 0.5	91.8 ± 0.3

Next, the TEM images of the PP-cp/EMA films are presented in Figure 6. For neat PP-cp [Fig. 6(a)], the ethylene copolymer formed round domains about 150–200 nm in diameter (a representative round domain is identified in a circle), and they

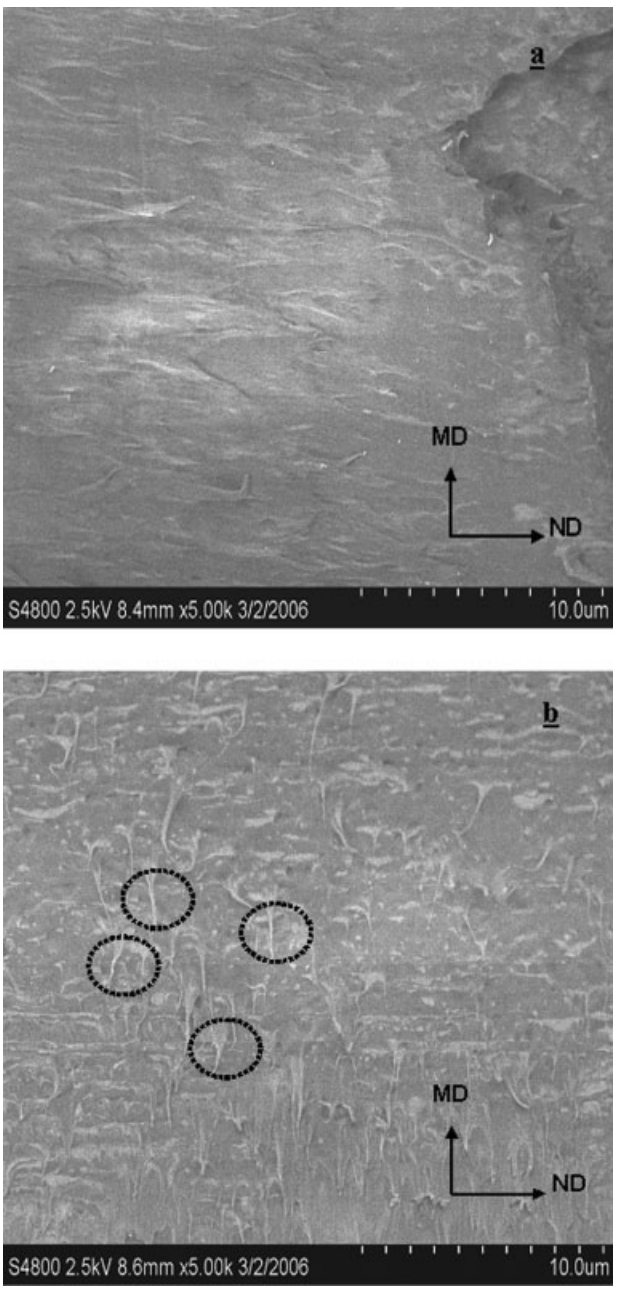

Figure 5 SEM micrographs of MD-ND plane of (a) Pure PP-cp film (b) PP-cp/15 wt % EMA blend film.

appear dark because of staining of the amorphous EPR phase.[44] Figure 6(b–d) shows the TEM images of 2 wt % EMA, 6 wt % EMA, and 15 wt % EMA blend films. In addition to the dark EPR domains, spotted domains of EMA are also observed. The EMA additive is well dispersed as elongated domains of 100–500 nm size (a representative elongated domain is identified in a rectangular box), which were distinctly visible at 6 wt % EMA and 15 wt % EMA blends. The EMA domains are well dispersed in the matrix even though no prior mixing step was used before blown-film extrusion. Since the EMA copolymer is semicrystalline, the domains were a combination of dark region (stained amorphous phase) with white spots (crystalline) within it, similar to that reported for nylon 66/SEBS copolymer blend.[45] For neat PP-cp film, the EPR domains appear more rounded (aspect ratio of 1–2). In contrast, the PP-cp/EMA blend films contain domains that are elongated (aspect ratio of 2–20). Further, as expected, the domains in 15 wt % EMA blend films were closer than those in 6 wt % blend films.

The formation of finely dispersed EMA domains can be partially attributed to the viscosity ratio of EMA to PP-cp. Figure 7 presents the viscosity results of neat EMA, neat PP-cp, and 15 wt % EMA blend. They exhibit a typical pseudoplastic behavior; shear thinning at shear rates higher than 0.01 s^{-1}. The viscosity of 15 wt % EMA blend was higher than that of pure PP-cp. This phenomenon has also been observed by Iannace et al.[17] during steady shear experiments on immiscible blends of PP and maleic-anhydride-functionalized ethylene copolymer and was attributed to phase-separated structure and molecular interaction. The zero-shear viscosity ratio ($\eta_{EMA}/\eta_{PP\text{-}cp}$) of EMA and PP-cp was found to be $\approx$0.4. The minimum particle size is typically observed near a viscosity ratio of 1.[20,46] The EMA droplets formed in the die were stretched in MD and TD due to the bubble blowing process. During cooling of the bubble, the freezing of the PP-cp matrix prevents these stretched EMA domains from reverting to round shape. Therefore, elongated domains can be seen distributed in the TD–ND cross section.

The importance of dispersed particle size,[25–28] interfacial adhesion,[26] and interparticle distance[29] on the tear behavior of the blends has been reported in the literature. Typically, a significant improvement in tear strength can be achieved when the particle size decreases below 1000 nm. In these studies, the dispersed domains were typically spherical, different from the elongated domains observed in our study. The role of shape and orientation of soft dispersed domains on the tear strength of films has not been thoroughly investigated in the literature. The soft EMA domains that appear somewhat wavy improved the energy dissipation during failure and led to an increase in MD and TD tear strengths for the blend films.

In addition, the presence of ethylene copolymer in PP-cp may have enhanced the interaction of PP-cp with EMA and assisted in better adhesion of the elastomers on the matrix polymer.[47] It is known that EMA is highly compatible with LDPE,[10] so the presence of ethylene phase in PP-cp may improve interaction of EMA with the matrix. Thus, if there is good interfacial bonding along with uniformly distributed elongated domains, there is better stress dis-

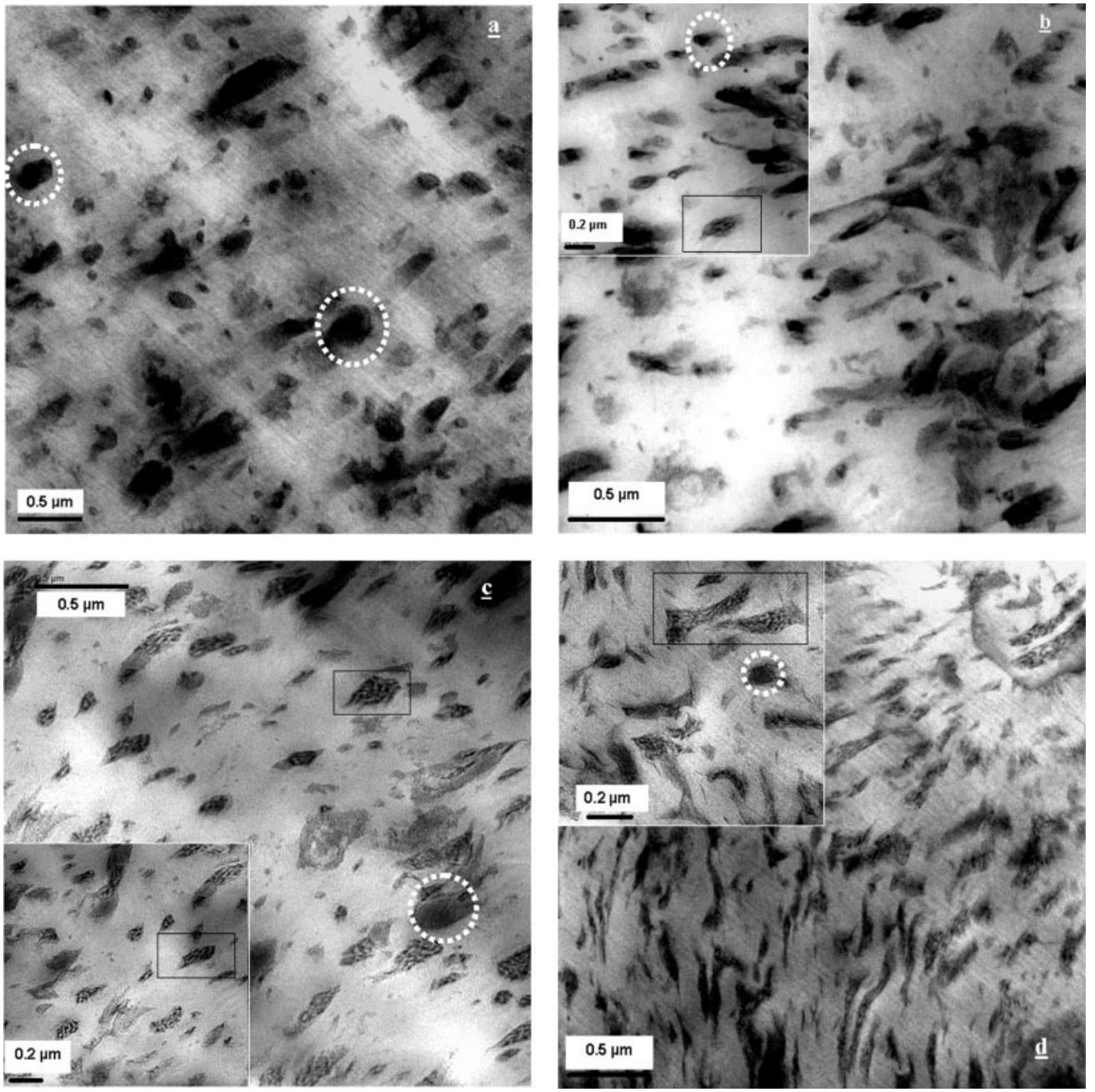

Figure 6 TEM micrographs of film sections from TD–ND plane: (a) Pure PP-cp, (b) PP-cp/2 wt % EMA, (c) PP-cp/6 wt % EMA, (d) PP-cp/15 wt % EMA.

tribution during tear, and the yielding zone is wider in the blend films, leading to increased tear resistance.

CONCLUSIONS

The tear strength of PP-cp/EMA blown films was examined in this work relative to their morphology. Although orientation and crystallinity of PP-cp matrix was not significantly affected by the addition of EMA dispersed phase, the tear strength of blend PP-cp films showed a significant increase with the addition of EMA. Morphological observations revealed good dispersion of EMA domains in the PP-cp matrix with elongated domains for 6 wt % and higher wt % EMA. The elongated rubbery EMA domains in the PP-cp matrix led to enhanced energy dissipation, which helps in explaining the increase in the tear strength.

The authors would like to acknowledge Dr. Joan Hudson and Mr. Amar Kumbhar at the electron microscopy facility at Clemson University for assisting in TEM. We are thank-

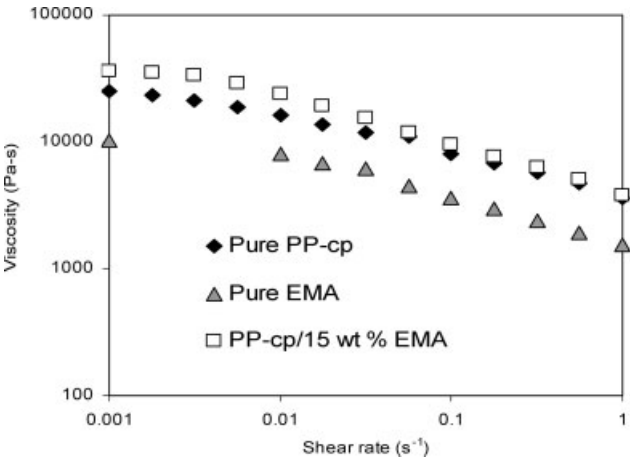

Figure 7 Low shear viscosity curves for pure PP-cp, pure EMA, and 15 wt % EMA at 240°C.

ful to Dr. Barbara Wood of DuPont Company for valuable suggestions regarding RuO_4 staining procedure. Any opinions, findings, conclusions, or recommendations expressed in this article are those of the authors and do not necessarily reflect those of the National Science Foundation.

References

1. Kanai, T.; Campbell, G. A. Film Processing; Hanser: Cincinnati, 1999.
2. Lopez-Manchado, M. A.; Valle, M.; Sapunar, R.; Quijada, R. J Appl Polym Sci 2004, 92, 3008.
3. D'Orazio, L.; Mancarella, C.; Martuscelli, E.; Sticotti, G.; Cecchin, G. J Appl Polym Sci 1999, 72, 701.
4. Ishikawa, M.; Sugimoto, M.; Inoune, T. J Appl Polym Sci 1996, 62, 1495.
5. Ramirez-Vargas, E.; Medelin-Rodriguez, F. J.; Navarro-Rodriguez, D.; Avila-Orta, C. A.; Solis-Rosales, S. G.; Lin, J. S. Polym Eng Sci 2002, 42, 1350.
6. Baker, G. L.; Buesinger, R. F. In Retec Polyolefins (V), Fifth International Conference on Polyolefins, Society of Plastics Engineers, Brookfield Center, CT, 1987; p 603.
7. Isik-Yuruksoy, B.; Senel, S.; Guven, O. J Therm Anal 1997, 48, 783.
8. Genovese, A.; Shanks, R. A. J Appl Polym Sci 2003, 90, 175.
9. Genovese, A.; Shanks, R. A. Macromol Mater Eng 2004, 289, 20.
10. Santra, R. N.; Samantaray, B. K.; Bhowmick, A. K.; Nando, G. B. J Appl Polym Sci 1993, 49, 1145.
11. Ana-Lucia, N. D. S.; Marisa, C. G. R.; Lea, L.; Beatriz, S. C.; Fernanda, M. B. C. J Appl Polym Sci 2001, 81, 3530.
12. Marguerat, F.; Carreau, P. J.; Michel, A. Polym Eng Sci 2002 42, 1941.
13. D'Orazio, L.; Mancarella, C.; Martuscelli, E.; Sticotti, G. J Mater Sci 1991, 26, 4033.
14. Oksuz, M.; Eroglu, M. J Appl Polym Sci 2005, 98, 1445.
15. Wu, S. Polymer 1985, 26, 1855.
16. Yong, W.; Zhang, Q.; Na, B.; Du, R.; Fu, Q.; Shen, K. Polymer 2003, 44, 4261.
17. Yingwei, Di.; Iannace, S.; Nicolais, L. J Appl Polym Sci 2002, 86, 3430.
18. Maciel, A.; Salas, V.; Manero, O. Adv Polym Technol 2005, 24, 241.
19. Hongzhi, L.; Tingxiu, X.; Lianlong, H.; Yuchun, O.; Guisheng, Y. J Appl Polym Sci 2006, 99, 3300.
20. Serpe, G.; Jarrin, J.; Dawans, F. Polym Eng Sci 1990, 30, 553.
21. Paul, S.; Kale, D. D. J Appl Polym Sci 2000, 76, 1480.
22. Zhang, X. M.; Elkoun, S.; Ajji, A.; Huneault, M. A. Polymer 2004, 45, 217.
23. Cherukupalli, S.; Gottlieb, S. E.; Ogale, A. A. J Appl Polym Sci 2005, 98, 1740.
24. Yuksekkalayci, C.; Yilmazer, U.; Orbey, N. Polym Eng Sci 1999, 39, 1216.
25. Chauyjuljit, S.; Moolsin, S.; Potiyaraj, P. J Appl Polym Sci 2005, 95, 826.
26. George, S.; Prasannakumari, L.; Koshy, P.; Varughese, K. T.; Thomas, S. Mater Lett 1996, 26, 51.
27. Kunz-Douglas, S.; Beaumont, P. W. R.; Ashby, M. F. J Mater Sci 1980, 15, 1109.
28. Kumar, C.; George, K. E.; Thomas, S. J Appl Polym Sci 1996, 61, 2383.
29. Ndiba, D. Presented at ANTEC 1998, Proceedings of the 56th Annual Technical Conference, Society of Plastics Engineers, Atlanta, GA, 1998.
30. Takashige, M.; Kanai, T.; Yamada, T. Int Polym Process 2004, 19, 147.
31. Gebreselassie, G.; Starling, M.; Khambete, S.; Tompson, G. U.S. Pat. 6,710,133 (2004).
32. Stein, R. S. J Polym Sci 1957, 24, 383.
33. Nielson, A. S.; Batchelder, D. N.; Pyrz, R. Polymer 2002, 43, 2671.
34. Lu, J.; Sue, H.; Rieker, T. J Mater Sci 2000, 35, 5169.
35. Chang, A. C.; Chum, S. P.; Hiltner, A.; Baer, E. Polymer 2002, 43, 4923.
36. Coran, A. Y.; Patel, R. J Appl Polym Sci 1976, 20, 3005.
37. Ibnelwaleed, A. H.; Rehan, A. C.; Basel, F. A. Polym Eng Sci 2004, 44, 2346.
38. Granado, A.; Eguiaza'bal, J. I.; Naza'bal, J. J Appl Polym Sci 2004, 91, 132.
39. Chang, A. C.; Chum, S. P.; Hiltner, A.; Baer, E. Polymer 2002, 43, 6515.
40. Chang, A. C.; Inge, T.; Tau, L.; Hiltner, A.; Baer, E. Polym Eng Sci 2002, 42, 2202.
41. Montoya, M.; Abad, M. J.; Barral Losada, L.; Bernal, C. J Appl Polym Sci 2005, 98, 1271.
42. Oommen, Z.; Thomas, S. J Appl Polym Sci 1997, 65, 1245.
43. Papadopoulou, C. P.; Kalfoglou, N. K. Polymer 1999, 41, 2543.
44. Nysten, B.; Ghanem, A.; Costa, J.-L.; Legras, R. Polym Int 1999, 48, 334.
45. Wood, B. A. Advances in Polymer Blends and Alloys Technology; Technomic: Lancaster, PA, 1992; Vol. 3, p 24.
46. Gonzalez-Nunez, R.; Favis, B. D.; Carreau, P. J.; Lavallee, C. Polym Eng Sci 1993, 33, 851.
47. Arjunan, P.; Kusznir, R. B. U.S. Pat. 5,281,651 (1994).